



Cite this: *Sustainable Energy Fuels*,
2025, 9, 4404

How do ambient conditions influence sorbent selection in adsorption-based direct air capture?[†]

Malte Glaser, ^a Arvind Rajendran ^b and Sean T. McCoy ^{*a}

The climate crisis is driving the urgent need to develop negative emission technologies, such as adsorption-based direct air capture (DAC), to combat global warming. Although DAC holds promise, it remains expensive and requires further technology innovation, design optimisation, and development of supply chains to scale up effectively and have a meaningful impact on climate. The performance of DAC is influenced by both local ambient conditions and the selection of sorbents. However, previous research typically evaluated DAC performance under constant ambient conditions and considered only a single sorbent per case study. This approach may result in an incomplete picture of DAC performance and suboptimal decision-making. Additionally, current DAC optimisation can be computationally expensive, making comprehensive global analysis impractical. Therefore, this study presents a computationally efficient, simplified, time-dependent, zero-dimensional (0-D) DAC model that accounts for multiple sorbents and hourly changing ambient conditions. The model is used to identify a sorbent that maximises net carbon removal by optimising for different geographical case studies to assess the impact of local, varying ambient conditions. The results demonstrate that DAC modelling can be simplified from a one-dimensional model to a 0-D model, thereby reducing computational demands. Additionally, beyond their absolute values, diurnal and seasonal variations in ambient temperature and humidity have a strong impact on sorbent performance. Key performance indicators, such as the net carbon removal rate, vary by up to 400% depending on the sorbent used or daily and seasonal variations in ambient conditions. Consequently, to improve DAC performance, sorbents should be selected based on ambient conditions. Finally, this study aims to advance the understanding of DAC and its role in mitigating climate change by providing general guidelines for DAC sorbent selection.

Received 14th May 2025
Accepted 16th June 2025

DOI: 10.1039/d5se00681c

rsc.li/sustainable-energy

1 Introduction

Global temperatures have risen by more than 1 °C since the late 19th century, largely attributed to the increasing concentration of CO₂ in the atmosphere.^{1,2} Reducing the atmospheric carbon dioxide (CO₂) concentration is one of the most difficult long-term challenges in climate change mitigation.^{3,4} Negative emission technologies (NETs), which include adsorption-based direct air carbon capture and storage (DACCS), therefore play an important role^{5,6} in attaining the objectives set forth by the Paris Agreement.⁷ DACCS extracts CO₂ from the atmosphere and permanently sequesters it, resulting in negative carbon emissions as long as the amount of greenhouse gases emitted during this process is less than that sequestered.^{8,9} Previous studies

examined the impact of ambient conditions on DAC and reported that factors such as temperature and relative humidity affect its performance.^{10–16} However, these studies often either assumed constant annual or monthly average ambient conditions, neglected diurnal variations, or considered changing conditions only during the evaluation of DAC performance, not during the optimisation. This assumption can become problematic for many high-latitude continental climate regions, such as Canada, where, for example, temperatures can vary from below −40 °C to above +30 °C throughout the year. Relying on average values in such cases does not adequately reflect the real-world conditions, as the variation in ambient conditions is excluded by averaging, potentially leading to inaccurate DAC analysis.

Moreover, optimising DAC performance is essential for the advancement of cost-effective DAC technology. While previous studies focused on optimising the cycle design of DAC processes (e.g., step duration, adsorption, and desorption settings), the process design (e.g., sorbent selection) was frequently assumed outside the scope of the study.^{13,16–20} Sorbents, however, are a fundamental element of DAC systems, as they capture (and release) CO₂. Various sorbents are being

^aDepartment of Chemical and Petroleum Engineering, University of Calgary, 2500 University Drive NW, Calgary, T2N 1N4, Alberta, Canada. E-mail: sean.mccoy@ucalgary.ca

^bDepartment of Chemical and Materials Engineering, University of Alberta, Donadeo Innovation Center for Engineering, 12th Floor, 9211 116 St NW, Edmonton, AB T6G 1H9, Alberta, Canada. E-mail: arvind.rajendran@ualberta.ca

[†] Electronic supplementary information (ESI) available. See DOI: <https://doi.org/10.1039/d5se00681c>



considered for DAC applications,^{21,22} each performing differently under varying ambient conditions. Thus, focusing on a single sorbent and excluding sorbent selection from the optimisation process may lead to suboptimal decisions.

Understanding the thermodynamics and performance of DAC is necessary for evaluating the impact of hourly changing ambient conditions on DAC's sorbent selection. Given the high cost and impracticality of observing real-world DAC performance today, computational modelling is indispensable for global analysis. Typically, the literature employs one-dimensional (1-D) models to describe DAC systems, addressing the co-adsorption of CO₂ and H₂O and providing results with both temporal and axial spatial resolution.^{23–26} 1-D models yield accurate results close to experimental measurements, but also require considerable computational resources, as they involve solving partial differential equations (PDEs) with corresponding initial and boundary conditions. While solving PDEs for a single case study is manageable, the computational demands escalate in global DAC screening, where process and cycle designs are optimised for hourly variations in ambient conditions across all geographical coordinates. This increase in complexity emphasises the need for more efficient, faster, yet accurate DAC modelling approaches. To reduce model complexity, it is argued that high axial resolution is unnecessary.²⁷ This arises because, to minimise pressure drop, most DAC models and patents in the literature^{26,28} assume shallow adsorption columns only a few centimetres deep. This shallow geometry limits the spatial scale of the model and leads to the proposal of a zero-dimensional (0-D) model, which ignores axial resolution. 0-D models for DAC were published previously;²⁹ however, these models are based on static assumptions, such as the system reaching equilibrium conditions instantaneously. Sorbents attain equilibrium loading when there is no net change in the amount of adsorbed molecules under the current conditions. The time required to reach equilibrium is influenced by heat and mass transfer within the system. As a result, depending on the cycle design, the sorbent may not be exposed to ambient air long enough to achieve equilibrium conditions. Current 0-D models do not account for this temporal dimension.

Therefore, the literature lacks three critical aspects: (a) the consideration of hourly changing ambient conditions in DAC modelling, (b) the integration of different sorbents into the optimisation problem, and (c) the availability of a fast and accurate time-dependent 0-D model to describe DAC thermodynamics. Consequently, the primary objective of this study is to examine how hourly changing ambient conditions affect sorbent selection in order to achieve optimal DAC performance. The second objective is to develop and explore the potential use of a time-dependent 0-D model for DAC modelling.

Bridging the gap between ambient conditions and sorbent selection advances the scientific understanding of DAC and offers practical solutions to guide policy and industry decisions for effective and strategic DAC deployment. Additionally, this study provides a foundational framework for future research. The use of the 0-D model makes DAC modelling more accessible to a broader audience, including those without access to high-

performance computing. Following the identification of optimal sorbent selection, subsequent studies can focus on further optimising DAC's process and cycle design under varying ambient conditions. This optimisation is important for developing sustainable, region-specific DACCS solutions, thereby improving the technology's applicability and ultimately contributing to climate change mitigation.

2 Modelling

To address the objectives of this study, a 0-D model with weather-dependent inputs is developed, validated, and optimised for targeted geographical case studies. The following section builds on a 1-D model presented in the literature,^{26,30} modified here by simplifying assumptions to reduce its complexity to a 0-D model and enable analysis of multiple sorbents. Unlike other 1-D models in the literature that focus on a single sorbent, Balasubramaniam *et al.*²⁶ examined three sorbents capable of co-adsorbing CO₂ and H₂O. Hence, to assist model validation, this study uses model parameters from Balasubramaniam *et al.*²⁶ This approach reduces the impact of differences in assumptions across studies regarding isotherms, kinetic data, and other parameters. In doing so, observed differences in performance are attributable to the sorbents themselves and their interactions with varying ambient conditions, making the data more suitable for the objectives of this study.

2.1 DAC model development

To describe the thermodynamics of DAC systems, most 1-D models represent the adsorption column as a packed bed. In contrast, the 0-D model developed in this study assumes that the adsorption column can be represented as a well-mixed reactor. This assumption is based on the fact that the shallow geometry of many modelled DAC columns often leads to uniform conditions throughout the column, both after the inlet and before the outlet. Mathematically, this means that the conditions within the adsorption column and at the outlet are identical. To achieve this, the process design features a single cylindrical adsorption column characterised by wall density ρ , length l , inner (in) and outer (out) radius r , and heat transfer coefficient h . The adsorption column is packed with sorbent particles, with detailed dimensions and parameters, such as the heat of adsorption ΔH_{ads} and specific heat capacity c_p , provided in Tables S1 and S2.† The sorbents studied that enable the co-adsorption of CO₂ and H₂O include APDES-NFC-FD-S (APDES),³¹ SIFSIX-18-Ni- β (SIFSIX),³² and NboFFIVE-1-Ni (NboFFIVE).³² These sorbents are selected to represent both amine-functionalised chemisorbents, which offer high CO₂ loadings but suffer from oxidative degradation, and physisorbents, which are more stable but sensitive to moisture. Nevertheless, it is assumed that all sorbents remain stable for the purposes of this analysis.

Fig. 1 illustrates the 0-D assumption and the chosen cycle design of the modelled temperature vacuum swing adsorption (TVSA) system. The TVSA cycle design involves four steps:



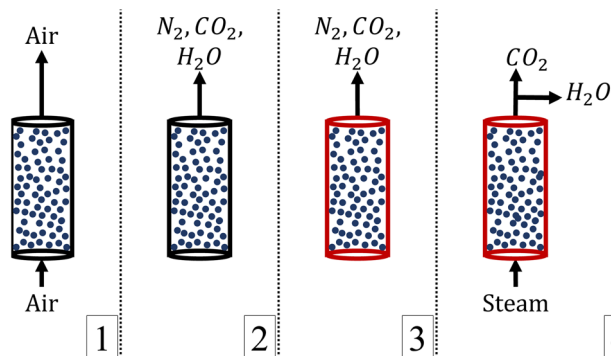


Fig. 1 Schematic representation of the four steps of the TVSA cycle: step 1—adsorption, during which ambient air enters the adsorption column. Step 2—evacuation, where residual gases are removed from the system until the desired desorption pressure is reached. Step 3—external heating, in which heat is supplied through a heating jacket (illustrated by red-coloured adsorption column walls) to raise the system temperature. Step 4—desorption, involving the continuous desorption of CO₂ and H₂O, followed by the separation of these gases to improve CO₂ purity.

adsorption (ads), evacuation (eva), heating (ht), and desorption (des). During the adsorption step, a fan blows air with ambient temperature T_{amb} and relative humidity ϕ_{amb} through the adsorption column. The fan overcomes the pressure drop of the adsorption column by applying power \dot{W}_{Fan} . Within the adsorption column, CO₂ and H₂O are adsorbed, while other gases are assumed not to interact with the sorbent. The air, which is leaner in CO₂ and H₂O, is then released back into the atmosphere. The evacuation step initiates the desorption process. The adsorption column inlet is closed, and a vacuum pump (VP) uses mechanical power \dot{W}_{VP} to evacuate the adsorption column until the desired desorption pressure p_{des} is attained, releasing the remaining gases into the atmosphere. During the heating and desorption steps, the temperature in the adsorption column is increased isobarically to the desorption temperature T_{des} by applying thermal energy \dot{Q}_{W} and additional mechanical power \dot{W}_{VP} . If desired, steam can be used during the desorption step to introduce an extra temperature and pressure swing, increasing productivity at the cost of higher energy consumption.²⁶ Temperature and pressure swings decrease the sorbent's equilibrium loading, causing the adsorbed CO₂ and H₂O to desorb. Continuous heating and the extraction of desorbed CO₂ and H₂O from the adsorption column maintain constant T_{des} and p_{des} . This ensures continuous desorption,

attained in the adsorption column. This process is repeated cyclically to continue capturing CO₂ from the air.

2.2 Simplified DAC model

The description of the 0-D model is based on three equations: molar balance, energy balance, and adsorption kinetics. The molar balance assumes that any moles \dot{n} of species $i \in \{\text{CO}_2, \text{H}_2\text{O}, \text{N}_2\}$ entering the adsorption column through the inlet (I) either exit (O) the system, adsorb (A) onto the sorbent, or accumulate (C) within the system (eqn (1)). The molar balance accounts for time τ , the universal gas constant R , the sorbent volume V_{sorbent} , the sorbent loading q_i^{A} , the adsorption column gas volume V^{C} , mole fraction y_i^{C} , pressure p^{C} , and temperature T^{C} .

$$\dot{n}_i^{\text{I}} - \dot{n}_i^{\text{O}} = \frac{\partial}{\partial \tau} \left[\frac{p^{\text{C}} \cdot V^{\text{C}}}{R \cdot T^{\text{C}}} \cdot y_i^{\text{C}} + q_i^{\text{A}} \cdot V_{\text{sorbent}} \right] \quad (1)$$

The temperature change in the adsorption column $\frac{\partial}{\partial \tau} T^{\text{C}}$ is determined using the energy balance shown in eqn (2). The energy balance accounts for the temperature difference between the inlet and adsorption column ($T_{\text{amb}} - T^{\text{C}}$), the pressure change in the system $\frac{\partial}{\partial \tau} p^{\text{C}}$, the heat of adsorption or desorption processes, external heat exchanges $\dot{Q}_{\text{external}}$, and sensible heat required to heat the mass m of sorbent (S), adsorbed, and accumulated gases. $\dot{Q}_{\text{external}}$ includes the heat exchanged through the adsorption column wall (W), considering the temperature difference between the adsorption column and its wall T^{W} (eqn (3)):

$$\begin{aligned} \frac{\partial}{\partial \tau} T^{\text{C}} = & \left(\sum \dot{n}_i^{\text{I}} \cdot c_{p,i}^{\text{I}} \cdot (T_{\text{amb}} - T^{\text{C}}) + V^{\text{C}} \cdot \frac{\partial}{\partial \tau} p^{\text{C}} \right. \\ & + \sum \Delta H_{\text{ads},i}^{\text{S}} \cdot \frac{\partial}{\partial \tau} q_i^{\text{A}} \cdot V_{\text{sorbent}} - \dot{Q}_{\text{external}} \left. \right) \\ & \cdot \left(m^{\text{S}} \cdot c_p^{\text{S}} + \sum q_i^{\text{A}} \cdot V_{\text{sorbent}} \cdot c_{p,i}^{\text{A}} + \sum n_i^{\text{C}} \cdot c_{p,i}^{\text{C}} \right)^{-1} \end{aligned} \quad (2)$$

$$\dot{Q}_{\text{external}} = h_{\text{in}} \cdot \pi \cdot r_{\text{in}} \cdot 2 \cdot l \cdot (T^{\text{C}} - T^{\text{W}}) \quad (3)$$

It is assumed that the adsorption column wall is instantaneously heated to the set desorption temperature during the heating and desorption steps.²⁶ In all other steps, however, the wall temperature varies according to the current temperature in the adsorption column and the ambient temperature, as shown in eqn (4).

$$\frac{\partial}{\partial \tau} T^{\text{W}} = \left(\frac{2r_{\text{in}}h_{\text{in}}}{r_{\text{out}}^2 - r_{\text{in}}^2} \cdot (T^{\text{C}} - T^{\text{W}}) - \frac{2r_{\text{out}}h_{\text{out}}}{r_{\text{out}}^2 - r_{\text{in}}^2} \cdot (T^{\text{W}} - T_{\text{amb}}) \right) \cdot (\rho^{\text{W}} \cdot c_p^{\text{W}})^{-1} \quad (4)$$

allowing the remaining adsorbed molecules to desorb until a new equilibrium is reached. After the desorption step, the inlet is opened to allow ambient air to flow in. This causes the system to cool and the overall pressure to rise until ambient conditions are

Adsorption isotherms are used to model the uptake of CO₂ and H₂O.³ Eqn (5) calculates the rate of adsorption or desorption by using a simple linear driving force (LDF) model, where $q_i^{\text{A},*}$ and



k_i represent the sorbent's equilibrium loading and each gas's mass transfer/LDF coefficient, respectively.

$$\frac{\partial}{\partial \tau} q_i^A = k_i \cdot (q_i^{A,*} - q_i^A) \quad (5)$$

The relative humidity in the adsorption column is determined by the ratio of the partial pressure of H_2O to its corresponding saturation pressure, the latter of which is calculated using the Clausius–Clapeyron equation. During the evacuation step (duration of τ_{eva}) the pressure change is assumed to follow an exponential profile, as detailed in eqn (6).

$$\frac{\partial}{\partial \tau} p^C = \frac{p^C}{\tau_{eva}} \log \left(\frac{p_{des}}{p^C} \right) \left(\frac{p_{des}}{p^C} \right)^{\frac{\tau}{\tau_{eva}}} \quad (6)$$

2.3 Productivity and energy calculations

The system's modelled productivity (Pr) can be determined by quantifying the amount of CO_2 desorbed $\Delta m_{CO_2, \tau_{des}}^A = \Delta m_{CO_2, cycle}$ during the duration of the desorption step τ_{des} and dividing it by the product of sorbent volume and cycle duration τ_{cycle} , as shown in eqn (7).

$$Pr = \frac{\Delta m_{CO_2, cycle}}{V_{sorbent} \cdot \tau_{cycle}} \quad (7)$$

To calculate the specific energy demand (SED) of the DAC system, it is necessary to factor in the absolute energy demand (AED) of the fan, vacuum pump, heating system, and, if applicable, steam generation. Although a 0-D model, by definition, does not account for pressure drop in the axial direction, differences in bed voidage among sorbents and their effects on the required fan power are adapted from published 1-D models.^{17,30} More specifically, the pressure drop in eqn (8) is calculated using Darcy's law in the axial direction, following the approach in Haghpanah *et al.*³⁰ In total, the energy required by the fan varies with the volumetric flow rate entering the system \dot{V}^I , the fan efficiency η_{Fan} , and the pressure drop across the adsorption column Δp .

$$\dot{W}_{Fan} = \frac{1}{\eta_{Fan}} \cdot \dot{V}^I \cdot \Delta p \quad (8)$$

The energy requirement of the vacuum pump (eqn (9)) varies with the adiabatic constant γ , pump efficiency η_{VP} , ambient pressure $p_{amb} = 1$ atm, and volumetric flow rate leaving the system \dot{V}^O .

$$\dot{W}_{VP} = \frac{1}{\eta_{VP}} \cdot \frac{\gamma}{\gamma - 1} \cdot \dot{V}^O \cdot p^C \cdot \left[\frac{p_{amb}^{\frac{\gamma-1}{\gamma}}}{p^C} - 1 \right] \quad (9)$$

A heating jacket supplies the necessary heat flux to reach the desorption temperature. \dot{Q}_w is calculated using the surface area of the adsorption column and the temperature difference between the adsorption column and the desorption temperature (eqn (10)).

$$\dot{Q}_w = h_{in} \cdot 2 \cdot \pi \cdot r_{in} \cdot l \cdot (T_{des} - T^C) \quad (10)$$

The energy demand for steam use is calculated using eqn (11) and accounts for the steam mass flow rate \dot{m}_{steam} , the difference between desorption temperature and saturation temperature

T_{sat} at the desorption pressure, an assumed water temperature of 5 °C and the heat of vaporisation $\Delta H_{vap, H_2O}$ which accounts for the phase change from liquid (l) to gaseous (g). Given the range of considered desorption pressures, T_{sat} is always greater than 5 °C, ensuring a positive temperature difference $T_{sat} - T_{5^\circ C}$.

$$\dot{Q}_{steam} = \dot{m}_{steam} \cdot (c_{p, H_2O, l} \cdot (T_{sat} - T_{5^\circ C}) + \Delta H_{vap, H_2O} + c_{p, H_2O, g} \cdot (T_{des} - T_{sat})) \quad (11)$$

By integrating the power demands over the entire cycle duration, the total primary SED can be determined (eqn (12)), assuming an efficiency of 50% for converting thermal to electrical energy.²⁶

$$SED = \frac{\int \dot{Q}_w + \int \dot{Q}_{steam} + 2 \cdot \left(\int \dot{W}_{Fan} + \int \dot{W}_{VP} \right)}{\Delta m_{CO_2, cycle}} \quad (12)$$

2.4 Integration of ambient conditions

To account for the influence of varying ambient conditions, particularly temperature and humidity, the 0-D model uses data sourced from NASA's MERRA-2 programme.³³ Hourly changing real-world ambient conditions for the year 2023 (totalling 8760 hours) are used as input to the model to identify the optimal sorbent for any given location.

However, NASA's dataset provides data for over 200 000 locations. Optimising the DAC process design for each location using hourly changing real-world ambient conditions would require substantial computational resources, potentially exceeding available capacities. This issue is addressed by temporally aggregating a year's worth of data into a select number of representative typical periods (TPs) and using these time series as input to the 0-D model to identify the optimal sorbent for each TP. Aggregating ambient conditions involves grouping days with similar weather patterns to define a representative typical day. These typical days are then organised into broader typical periods comprising multiple days with comparable ambient conditions; for example, June 1st and July 1st could be considered representative of a typical summer day in the northern hemisphere. However, these periods do not correspond directly to traditional seasons like winter, spring, summer, or autumn, since, for instance, a warm day in March might be grouped with one in October. Nevertheless, temporal aggregation allows for typical periods to be interpreted as analogous to typical seasons, potentially leading to DAC process designs that are tailored accordingly. The tsam library³⁴ in Python aggregates the data using a hierarchical aggregation algorithm.

One disadvantage of temporal aggregation is that the sequence of typical periods at a given location cannot be predetermined—such as TP2 always following TP1. To address this and capture inter-seasonal variations in ambient conditions, the data for an entire year is merged into a single time series which is then used as input to the 0-D model to identify the optimal sorbent. Since aggregating all 8760 hours into a single TP does not adequately represent diurnal and seasonal



Table 1 Summary of ambient conditions input

| Scenario | Purpose |
|-----------------------|----------------------------------|
| Actual | Accurate real-world analysis |
| Temporally aggregated | Intra-seasonal analysis |
| Resampled | (Faster) inter-seasonal analysis |
| Averaged | Literature benchmark analysis |

variations (as detailed in Section S.2†), the pandas library³⁵ in Python resamples the data for the entire year by averaging 20-hour intervals. This process reduces the number of modelled hours to 438. Additionally, changing the sorbent throughout the year to optimise DAC performance is considered impractical; therefore, a single optimal sorbent is selected for the entire year.

This study also explores scenarios with constant average ambient conditions in the 0-D model. This approach is intended to investigate whether using constant ambient conditions results in different optimal sorbents compared to those obtained under varying ambient conditions and to enable comparisons with previous studies. Table 1 summarises the various inputs for the four scenarios: actual, temporally aggregated, resampled, and averaged ambient conditions.

2.5 Model validation

The combination of molar balance, energy balance, and adsorption kinetics yields a set of coupled ordinary differential equations (ODEs) that necessitate a numerical solver to obtain their solution. The scipy package³⁶ in Python is used for this purpose. Subsequently, a specific DAC cycle design (*e.g.*, step duration, adsorption, and desorption settings) with given ambient conditions is modelled, yielding data on the variables listed in Table 2 at any given point in time. This data helps determine the model's key performance indicators (KPIs). To account for heating and cooling effects within the DAC system, the evaluation of the model's KPIs excludes the first cycle. KPIs of subsequent cycles are averaged over the duration of their respective cycles to ensure they are not influenced by the initial cold start.

Table 2 Output variables of the DAC model

| Variable | Description | Unit |
|-------------------------------------|---------------------------------------|------|
| $n_{\text{CO}_2}^{\text{A}}$ | CO ₂ sorbent loading | mol |
| $n_{\text{H}_2\text{O}}^{\text{A}}$ | H ₂ O sorbent loading | mol |
| $n_{\text{N}_2}^{\text{A}}$ | N ₂ sorbent loading | mol |
| $n_{\text{CO}_2}^{\text{C}}$ | CO ₂ in adsorption column | mol |
| $n_{\text{H}_2\text{O}}^{\text{C}}$ | H ₂ O in adsorption column | mol |
| $n_{\text{N}_2}^{\text{C}}$ | N ₂ in adsorption column | mol |
| $n_{\text{CO}_2}^{\text{O}}$ | Collected CO ₂ | mol |
| $n_{\text{H}_2\text{O}}^{\text{O}}$ | Collected H ₂ O | mol |
| $n_{\text{N}_2}^{\text{O}}$ | Collected N ₂ | mol |
| T^{C} | Temperature in adsorption column | K |
| p^{C} | Pressure in adsorption column | Pa |
| T^{W} | Wall temperature | K |

The 0-D model is validated against the 1-D model by comparing commonly used KPIs, specifically Pr and SED. Balasubramaniam *et al.*²⁶ reported their results for various cycle designs under a constant ambient temperature of 20 °C and a relative humidity of 50%. These same cycle designs and ambient conditions are used as input to the 0-D model. Comparing the computed KPIs from both models allows for an assessment of whether the 0-D model can be used for the purposes of this study.

2.6 Objective function

Pr and SED do not account for upstream emissions associated with DAC operation and, therefore, do not reflect the real negative emissions potential of a specific DAC sorbent under varying ambient conditions. To address this, Pr, defined per unit volume of sorbent, is converted into a unit of mass captured per unit time. This conversion is done by fixing the volume of the adsorption column, and consequently, the size of the DAC system, based on the dimensions stated in Table S1.† Additionally, SED is multiplied by the on-site greenhouse gas emissions ($\text{CO}_{2,\text{eq}}$) from the energy used $e_{\text{energy},\text{CO}_{2,\text{eq}}} = 0.184 \text{ kg kW}^{-1} \text{ h}^{-1} = 0.0511 \text{ kg MJ}^{-1}$,³⁷ which is assumed to originate from natural gas combustion. This conversion allows two new KPIs to be determined: removal rate (RR) and carbon removal efficiency (CRE).¹⁷ A high RR ensures the removal of large quantities of CO₂ by the DAC system within a short period of time (eqn (13)), while a high CRE minimises on-site emissions $\Delta m_{\text{CO}_2,\text{on-site}}$ resulting from DAC operation relative to the amount of CO₂ captured (eqn (14)).

$$\text{RR} = \frac{\Delta m_{\text{CO}_2,\text{cycle}}}{\tau_{\text{cycle}}} \quad (13)$$

$$\text{CRE} = \frac{\Delta m_{\text{CO}_2,\text{cycle}} - \Delta m_{\text{CO}_2,\text{on-site}}}{\Delta m_{\text{CO}_2,\text{cycle}}} \quad (14)$$

However, RR is typically inversely related to CRE, necessitating a trade-off and bi-objective optimisation, which in turn requires considerable computational resources. Bi-objective optimisation is avoided by introducing the net carbon removal rate (CRR)¹⁷ as the objective function, shown in eqn (15), and optimising CRR through single-objective optimisation. CRR accounts for the net amount of CO₂ removed from the atmosphere, considering both total CO₂ captured and CO₂ emitted to the atmosphere through on-site processes within a given time period. This objective function aligns with the goal of global carbon dioxide removal efforts while conserving computational resources.

$$\text{CRR} = \text{RR} \cdot \text{CRE} \quad (15)$$

2.7 Decision variables

Factors influencing CRR include the type of sorbent, which introduces an integer variable to the optimisation problem. However, each sorbent has unique characteristics. Therefore, as part of the overall cycle design, the duration of adsorption τ_{ads}



and desorption, desorption pressure, and air inlet velocity v_{ads} are also considered, adding four continuous variables. Optional steam desorption is included as a second integer variable, along with the corresponding steam inlet velocity v_{steam} as an additional continuous variable. Constraints for the decision variables considered are shown in Table S3.[†] This means that, for a given input of ambient conditions, a single optimal sorbent and its corresponding set of cycle design variables are determined, both of which remain fixed throughout the specified time period. Consequently, each input of ambient conditions can result in a different sorbent and different set of fixed cycle design variables. Optimising the cycle design variables for each individual cycle would better accommodate hourly changing ambient conditions. However, this approach lies beyond the scope of this study, as addressing it would effectively transform the problem into a control optimisation challenge. Table S4[†] lists parameters of the cycle design that are assumed to remain constant during optimisation. These parameters either have little impact on DAC performance or serve to simplify the complexity of the optimisation problem. Given the non-linearity and integer nature of the optimisation, particle swarm algorithm (PSA) is employed for its effectiveness in solving such problems. The pymoo package³⁸ in Python applies PSA to the DAC model, employing 10 000 particles until the algorithm converges to ensure an optimal solution is reached, as detailed further in Section S.3.[†]

2.8 Case studies

The 0-D model, integration of ambient conditions, and optimisation approach establish a framework that allows for the rapid and straightforward investigation of how ambient conditions influence the optimal sorbent selection for DAC. This framework can be applied to any location, provided data on ambient conditions is available, enabling a global analysis of DAC systems. As an example, the framework is demonstrated through two case studies: Calgary and Barbados. These locations are chosen due to their diverse climates, spanning cold and dry winters to warm and humid summers, to best demonstrate the effects of varying sorbent performance.

In each case study, the model is optimised across several scenarios using the four different inputs of ambient conditions detailed in Section 2.4 and Table 1: the actual real-world data, each typical period's aggregated data, resampled data, and constant average data. In each scenario, one of the four inputs of ambient conditions is used, modelling one hour at a time. Results from each modelled hour serve as initial conditions for the subsequent hour, with ambient conditions updated based on the scenario investigated. PSA maximises CRR using the decision variables outlined in Table S3,[†] determining the optimal sorbent for the given input of ambient conditions, while maintaining a CO₂ purity greater than 95%.

3 Results and discussion

First, the rationale for transitioning from a 1-D to a 0-D model for DAC modelling is explained. Second, the optimal sorbent for

different ambient conditions is discussed. Following this, the impact of ambient condition variability along with the effects of on-site energy emissions on sorbent selection are analysed.

3.1 Rationale for simplified DAC models

Fig. 2 compares the KPI results of the 0-D and 1-D model for various steam-assisted cycle designs using APDES sorbent. The KPIs from the 0-D model follow the same trend as those from the 1-D model, albeit with a slight shift. The difference is due to errors introduced by the effects of conduction, convection, and dispersion in energy and molar balances, for which the 0-D model cannot accurately account. Introducing a constant sorbent-specific calibration factor into the 0-D model mitigates this difference, bringing it into better alignment with the 1-D model. The agreement between the calibrated 0-D model and the 1-D model is quantified by the R^2 value, which is sufficiently high for the purposes of this study. While the calibration factor has no physical meaning, it is applied to ensure the best possible alignment with previously published 1-D models. Accordingly, the calibrated model is used for the analysis in the following sections.

For the same process design as above, Fig. 3 illustrates the temporal trajectories of CO₂ loading, H₂O loading, and the temperature in the adsorption column, with cycle design parameters detailed in Table 3. The trajectories closely resemble those published by Balasubramaniam *et al.*,²⁶ confirming that the 0-D and 1-D models produce nearly identical results. The figure illustrates that H₂O reaches its equilibrium loading much faster than CO₂, consistent with the assumption by Balasubramaniam *et al.*²⁶ that the mass transfer coefficient of H₂O is 1000 times greater than that of CO₂. In fact, because CO₂ mass transfer is slow, CO₂ never fully reaches equilibrium loading for this particular cycle design. In real-world scenarios, both mass

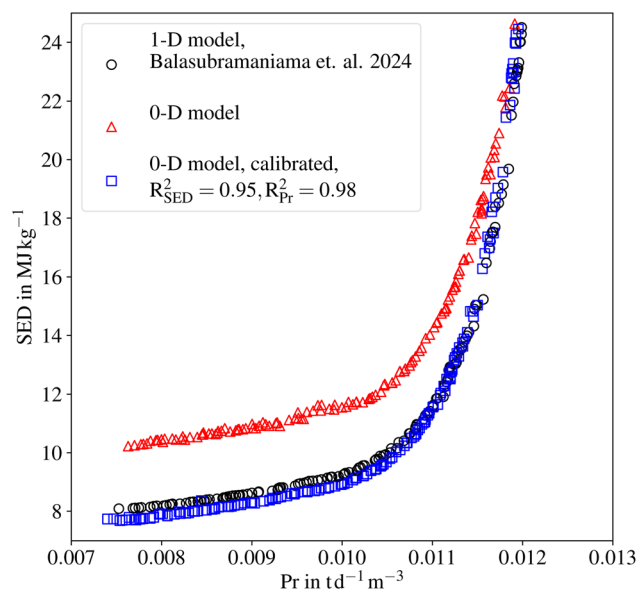


Fig. 2 Comparison of calculated specific energy demand (SED) and productivity (Pr) for various steam-assisted cycle designs using APDES sorbent, between 1-D model, 0-D model, and calibrated 0-D model.



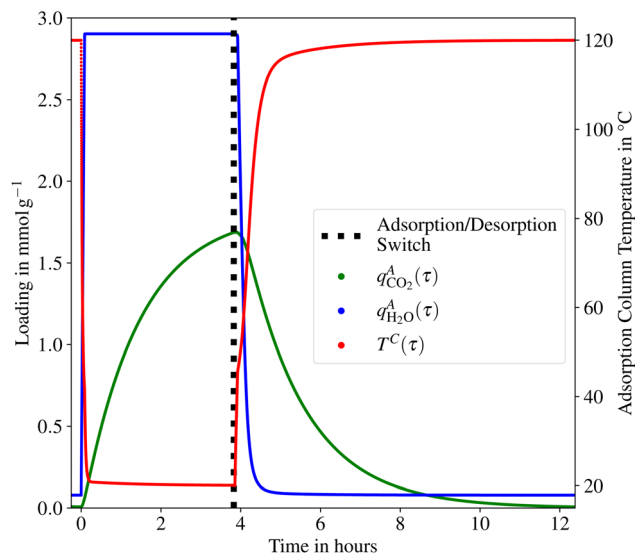


Fig. 3 Temporal trajectories of adsorption column temperature T^C , CO_2 loading $q^A_{\text{CO}_2}$, and H_2O loading $q^A_{\text{H}_2\text{O}}$ illustrating their variation over time in the adsorption column under fixed ambient conditions ($T_{\text{amb}} = 20^\circ\text{C}$ and $\phi_{\text{amb}} = 50\%$).

Table 3 Cycle design parameters for validation purposes²⁶

| Parameter | Description | Value | Unit |
|---------------------|--------------------------|--------|-------------------|
| τ_{ads} | Adsorption step duration | 13 772 | s |
| τ_{eva} | Evacuation step duration | 100 | s |
| τ_{ht} | Heating step duration | 704 | s |
| τ_{des} | Desorption step duration | 30 000 | s |
| T_{des} | Desorption temperature | 120 | K |
| p_{des} | Desorption pressure | 5000 | Pa |
| v_{ads} | Air inlet velocity | 0.1081 | m s^{-1} |
| v_{steam} | Steam inlet velocity | 0.0541 | m s^{-1} |

transfer coefficients would vary over time due to the dynamics and conditions within the adsorption column. However, due to a lack of data, these values are assumed to remain constant. The influence of the mass transfer coefficient of H_2O is further examined in Section S.4,[†] confirming that the findings of this study remain robust across a broad range of values. In addition, the figure depicts a rapid decrease in temperature close to ambient conditions of $T_{\text{amb}} = 20^\circ\text{C}$ (at $\phi_{\text{amb}} = 50\%$) at the beginning of the adsorption step. However, ambient conditions are only reached once fewer molecules adsorb, thereby reducing the small effect of the heat of adsorption. After the evacuation step, the temperature rises until it reaches the desorption temperature. The fact that adsorption, desorption, and heating occurs over time emphasises the advantage of a time-dependent 0-D model over previous static 0-D models, particularly when slow kinetics prevent the system from reaching equilibrium, making the assumption of immediate equilibrium not applicable.

In conclusion, while reducing a PDE system to an ODE system may compromise accuracy, the unique design of the DAC adsorption column allows for this simplification without considerable loss of precision. As a result, although the 0-D

model lacks spatial resolution within the adsorption column, its primary KPIs align closely with those of the 1-D model. While a more detailed model is preferable for in-depth analysis, this simplification is reasonable for the purposes of this study.

3.2 Effect of varying ambient conditions on DAC

Fig. 4 illustrates the impact of varying ambient conditions on DAC performance, with the stepwise trajectory resulting from the assumed hourly changes. It uses the cycle design parameters described in Table 3, APDES as the sorbent, and artificial sinusoidal ambient conditions for demonstration purposes. The figure suggests that variations in ambient relative humidity during the adsorption step correlate with variations in the amount of H_2O adsorbed. Specifically, an increase in relative humidity (see hours 1 to 4) leads to higher H_2O adsorption by the sorbent, while a decrease (hours 13 to 16) results in lower H_2O adsorption. Since the adsorption step is the only step in which the DAC system interacts with ambient air, Fig. 4 suggests that ambient conditions during adsorption have the greatest influence on sorbent performance. Consequently, assuming constant ambient conditions in DAC modelling does not accurately reflect *in situ* performance.

The analysis in Fig. 4 also demonstrates that the timing of starting DAC operation influences overall performance. For instance, starting the cycle five hours later would result in different values for SED, Pr, and CRR, with respective differences of 1.3%, -2.7% , and 0.11% for the shown cycles. However, while this effect is noticeable when considering only

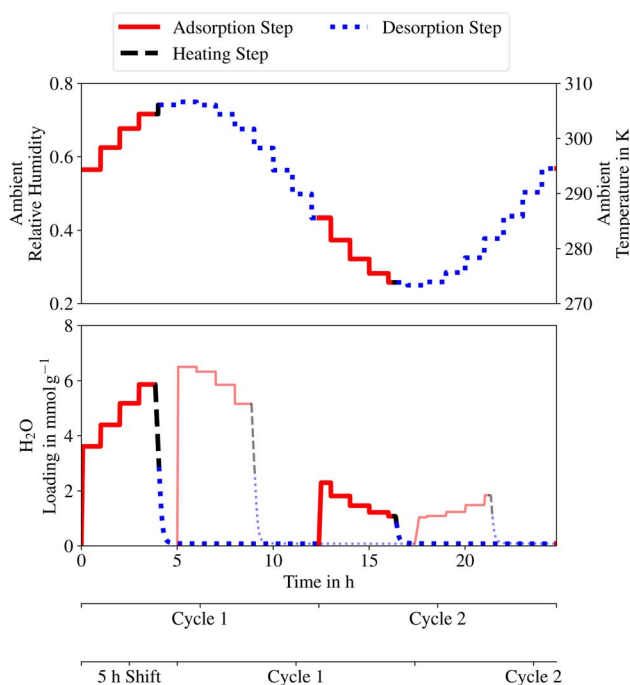


Fig. 4 Comparison of an artificial ambient temperature and relative humidity trajectory and corresponding H_2O loading across the adsorption, heating, and desorption steps of two DAC cycles. The evacuation step is not visible as it is too short. The semi-transparent and thinner line represents the same cycle, started five hours later.

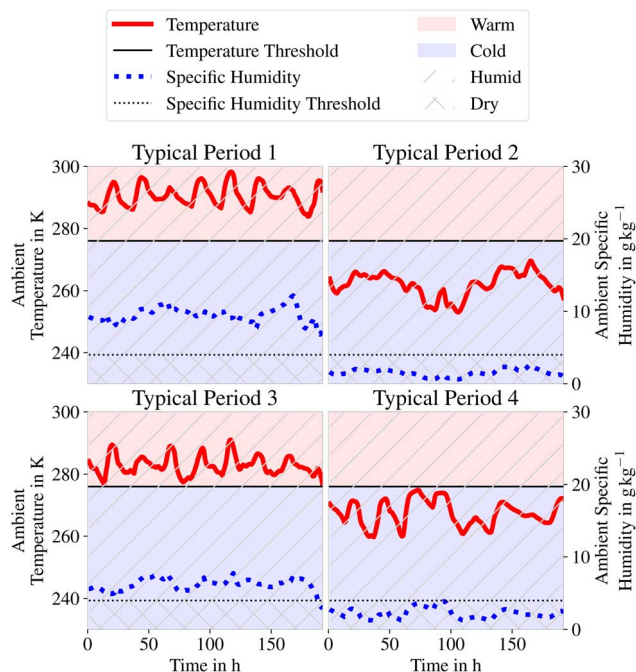


Fig. 5 Ambient temperature and specific humidity (wet basis) across four typical periods in Calgary, with thresholds characterising warm/cold and humid/dry conditions.

a few cycles, its impact becomes negligible as the analysis includes several hundred cycles (as is typical in a year). This is because, in the real world, ambient conditions do not follow a clear 24-hour cycle, making the described effects less pronounced.

3.3 Optimal sorbent selection for different typical periods

Analysis of temporal aggregation results in Calgary suggests that using four typical periods, each spanning eight days, accurately reflects real-world data while reducing the modelled hours from 8760 to 768 (see Section S.2† for further information). Using four TPs also enables the definition of four distinct typical seasons within a year. However, instead of categorising by months as is typically done, this approach groups days with similar ambient conditions into one of the four seasons. The results of this aggregation are illustrated in Fig. 5, where a thin solid and dotted line divide the subplot into two regions, marking a visualisation threshold that separates warm, cold, humid, and dry conditions. Ultimately, this method enables the identification of an optimal sorbent for each typical period.

Table 4 shows the optimal sorbent for maximising CRR in each typical period in Calgary. TP1 and TP3 favour APDES, while TP2 and TP4 favour SIFSIX. The results further demonstrate that ambient conditions above the threshold lines in Fig. 5—characterised as warm and humid—favour the use of APDES, whereas ambient conditions below this line (cold and dry) favour SIFSIX. Together, the above findings demonstrate the impact of ambient conditions on sorbent performance and suggest that tailoring sorbent selection accordingly could improve DAC performance. Although changing sorbents in response to each TP may be challenging in practice, these

Table 4 Optimal sorbent selection for different typical periods (TPs) and their corresponding characterised ambient conditions (AC)

| TP | Characterised AC | Optimal sorbent |
|----|------------------|-----------------|
| 1 | Warm & humid | APDES |
| 2 | Cold & dry | SIFSIX |
| 3 | Warm & humid | APDES |
| 4 | Cold & dry | SIFSIX |

results offer preliminary guidelines for optimising sorbent selection based on ambient conditions to achieve better DAC performance.

To further illustrate the effect of ambient conditions on sorbent performance, Fig. 6 depicts the quantitative differences in CRR among various sorbents under identical cycle designs and ambient conditions (TP1 and TP2). The results demonstrate that CRR varies with the sorbent used, emphasising the critical importance of sorbent selection in DAC process design. Specifically, employing APDES over SIFSIX in TP1 increases CRR by 158%, while using SIFSIX instead of APDES in TP2 increases CRR by 404%. However, it should be noted that the cycle design used is not optimised, so the observed difference might be smaller if optimised cycle designs were applied for each sorbent. Optimising the cycle design is, however, beyond the scope of this study. Additionally, the figure indicates that NboFFIVE is not recommended for use in Calgary under these ambient conditions, as it never yields a positive CRR. This is because the ambient conditions in all TPs are unfavourable; using NboFFIVE demands excessive energy and leads to considerable on-site emissions, while capturing insufficient CO₂, rendering DAC operation impractical.

The absolute values shown in Fig. 6 help to contextualise the results discussed above. Since this study models only a single adsorption column, with its dimensions fixed, the amount of CO₂ removed is relatively small. Previous studies^{17,26} addressed the scaling up of their models by multiplying their system's performance with a constant factor to align with industrial capacities. However, this approach is not considered here for two reasons. Firstly, scaling up does not affect the qualitative results of this study, which aims to evaluate sorbent selection under different ambient conditions; thus, the sorbent choice remains unchanged as the system scales. This consideration becomes more important when taking into account the life-cycle emissions and costs of the entire DAC system, which are beyond the scope of this study. Secondly, these studies^{17,26} used Climeworks' Orca plant as a reference system, citing their target of capturing 4000 t of CO₂ per year. However, Climeworks recently reported³⁹ that their actual performance falls far below the initially targeted 4000 t, making any scale-up based on proposed industry data challenging.

The varying performance of APDES and SIFSIX under different ambient conditions can be attributed to their distinct underlying chemistries. APDES and SIFSIX represent two different types of sorbents: a chemisorbent and a physisorbent, respectively. Physisorption relies on physical forces, such as van der Waals forces, to capture molecules, while chemisorption involves the formation of chemical bonds. These fundamental



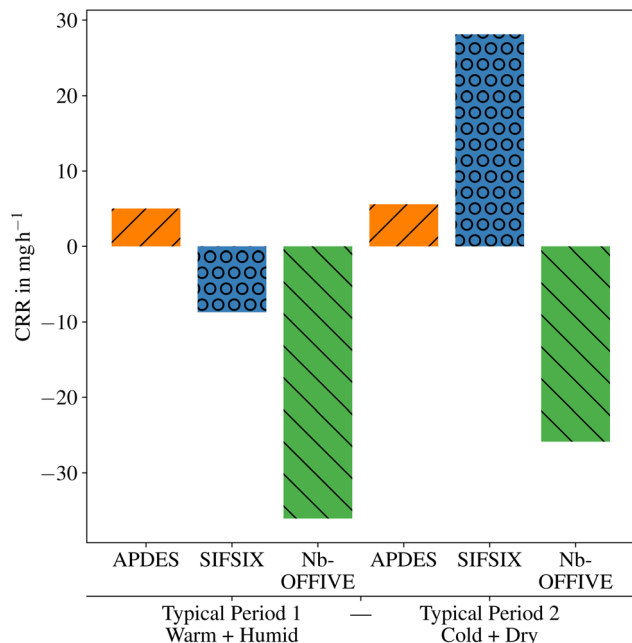


Fig. 6 Comparison of net carbon removal rates (CRR) achieved with APDES, SIFSIX, and NbOFFIVE under identical cycle designs and ambient conditions, using typical periods 1 (warm and humid) and 2 (cold and dry) in Calgary as representative examples.

differences result in distinct behaviours when exposed to H_2O , which in turn affect the CO_2 adsorption performance of each sorbent under varying humidity levels. APDES, a chemisorbent, promotes synergistic adsorption of both CO_2 and H_2O , improving its performance in humid conditions. Conversely, SIFSIX, a physisorbent, faces competitive adsorption between CO_2 and H_2O , as elaborated further in Section S.1.† Thus, in humid environments, the prevalence of H_2O hinders the effectiveness of SIFSIX by occupying the adsorption sites that would otherwise be available for CO_2 . In contrast, in dry conditions, the reduced presence of H_2O lowers this competition, allowing SIFSIX to perform better. Hence, the prevalence of H_2O in ambient air, its adsorption, and subsequent desorption determines which sorbent performs best. This is because desorbing H_2O consumes energy and subsequently causes on-site emissions. For CRR optimisation, it is reasonable to use more energy for H_2O desorption only if the system captures more CO_2 as a result. Conversely, the less CO_2 the system captures relative to the amount of H_2O it captures, the less beneficial the DAC operation becomes, as the additional on-site energy emissions cannot be offset by more CO_2 captured. While these results already demonstrate the impact of ambient temperature and humidity on sorbent selection, further analysis is needed to explain how variations in these ambient conditions impact the overall performance of the DAC system.

3.4 Influence of ambient condition variability on sorbent selection

Fig. 7 illustrates the actual, resampled, and average temperature and humidity data for Calgary and Barbados. It demonstrates

that Calgary experiences strong diurnal and seasonal variations in ambient conditions, while Barbados remains relatively stable throughout the year. Those inter-seasonal changes in Calgary, however, are not accounted for in the previous analysis in Section 3.3. Therefore, using both the actual and resampled data, the results in Fig. 7 indicate that Calgary, with its cold, dry, and varying ambient conditions, favour SIFSIX, while Barbados, being warm, humid, and stable, favour APDES. This aligns with the previous finding for Calgary's TPs alone. Also, the optimal sorbent remains the same regardless of whether actual or resampled ambient conditions are used. Thus, in this case, using resampled data accounts for inter-seasonal variations while saving computational resources. In fact, it can reduce computational time by up to 90% compared to processing all 8760 hours. Subsequently, this can allow for a global analysis of DAC systems by enabling comparisons across different locations to assess whether ambient conditions influence the choice of optimal sorbents.

The results further demonstrate that assuming constant ambient conditions may result in suboptimal sorbent selection and poor decision-making in practice, as APDES is identified as the best option in both locations under these ambient conditions. This demonstrates that, in a location like Barbados, where ambient conditions are relatively stable, assuming constant ambient conditions does not affect the choice of optimal sorbent, and the use of average ambient conditions for

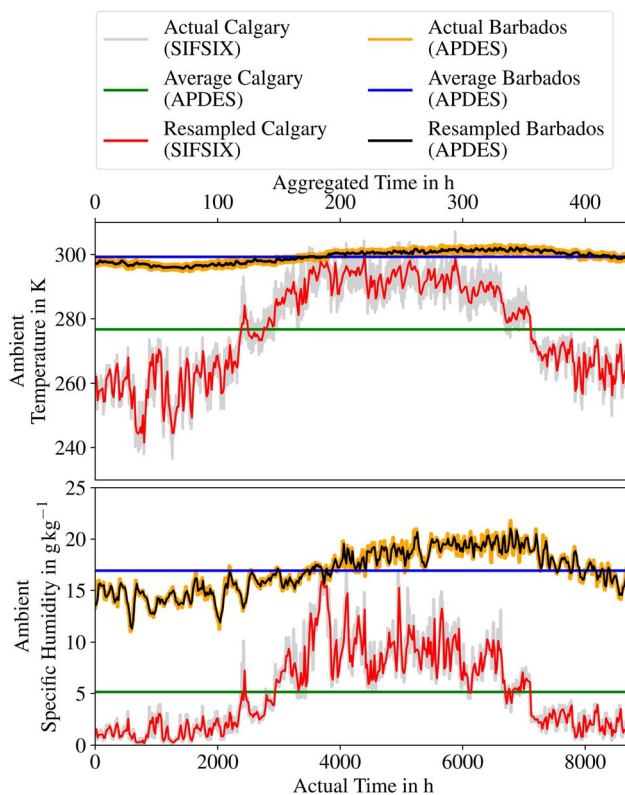


Fig. 7 Comparison of actual, resampled, and average ambient temperature and specific humidity for Calgary and Barbados, along with the corresponding optimal sorbent.



Table 5 Range of artificial ambient conditions considered

| Variable | Range | Increments | Unit |
|---------------------|---------|------------|------|
| Temperature | 250–350 | 5 | K |
| Relative humidity | 0–0.95 | 0.05 | — |
| Relative variations | 0–0.9 | 0.3 | — |

optimisation does not lead to suboptimal decisions. However, in a location with varying ambient conditions like Calgary, assuming constant ambient conditions, as commonly done in the literature thus far, leads to suboptimal decisions and does not provide the best possible process design for DAC.

The impact of sorbent choice on model performance and KPIs is analysed in greater detail in Section S.6.† The analysis demonstrates that selecting APDES over SIFSIX in Calgary and SIFSIX over APDES in Barbados considerably affects CRR, SED, and the capture of CO₂ and H₂O, with implications that may even result in net-positive emissions for DAC. It also emphasises the strong dependence of ambient conditions on KPIs and their variability, challenging the applicability of fixed benchmark KPI values commonly used or reported in the literature. As an example, for two different locations (Calgary and Barbados) with two different sorbents (APDES and SIFSIX), CRR and SED can vary by up to 476% and 159%, respectively, while even within the same location, such as Calgary, these KPIs can change by 150% and 33% over just a few cycles, particularly when ambient conditions vary strongly.

Hence, it is not only the ambient temperature and humidity but also their relative variations that influence DAC performance and optimal sorbent selection. While specific results can only be obtained if the actual real-world ambient conditions for a given location are used as input to the model, this study provides general guidelines for DAC sorbent selection. To achieve this, artificial ambient conditions are used to represent the full range of ambient conditions, as detailed in Section S.5† and Table 5. Fig. 8 and 9 illustrate the normalised achievable CRR and optimal sorbent selections across various combinations of temperature, relative humidity, and relative variation, emphasising that colder and drier ambient conditions typically result in higher CRR, while greater variation in ambient conditions also tends to increase CRR. The results further indicate that SIFSIX and NboFFIVE are preferred under cold and dry conditions, whereas APDES is favoured under warm and humid conditions. However, at cold temperatures, even a low specific humidity can result in high relative humidity due to the low saturation pressure of H₂O at these temperatures. Therefore, the ambient conditions for optimal use of SIFSIX and NboFFIVE can be further detailed: SIFSIX is preferred in cold and dry conditions which still result in high relative humidity, whereas NboFFIVE is the better choice in ambient conditions that are even drier, where relative humidity remains low despite the cold temperatures. This is consistent with the previous findings for Calgary's ambient conditions, where SIFSIX is preferred, as the cold temperatures in Calgary during those periods mean that relative humidity is still reasonably high (always >25%), explaining the preference for SIFSIX over NboFFIVE. Fig. 9 also

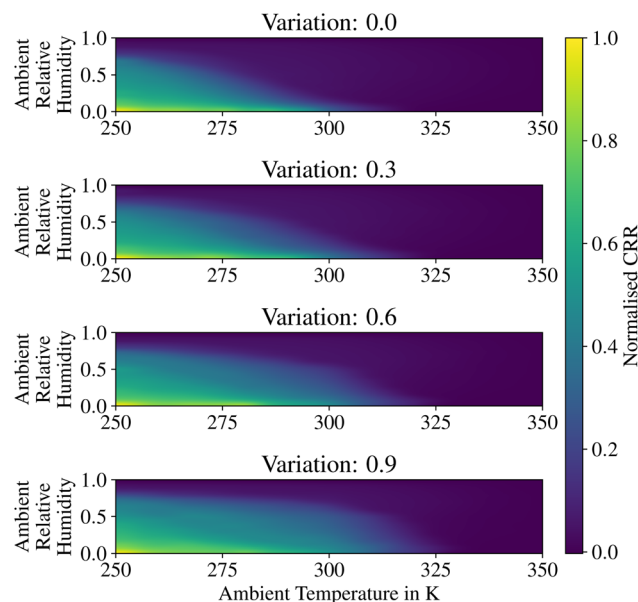


Fig. 8 Heatmap showing the normalised achievable net carbon removal rate (CRR) based on ambient temperature, relative humidity, and their relative variations.

demonstrates the effect of relative variations in ambient conditions on sorbent selection, suggesting that SIFSIX and NboFFIVE may be beneficial in ambient conditions with warm and humid averages, provided there are considerable relative variations. This implies that the sorbent is occasionally exposed to cold and dry conditions, emphasising the complexity of the problem and the inadequacy of considering average ambient conditions alone during the decision-making process. Although

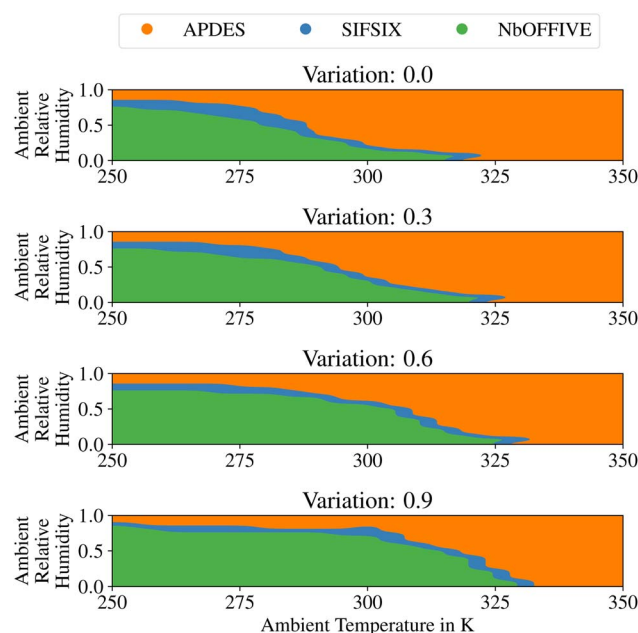


Fig. 9 Heatmap showing the optimal sorbent based on ambient temperature, relative humidity, and their relative variations.



this analysis currently accounts for only a select number of sorbents and artificial ambient conditions, it provides a straightforward heuristic for selecting the best sorbent based on average temperature, relative humidity, and relative variations in ambient conditions at a specific location. While including more sorbents would increase the variety of solids, it is unlikely to improve the reliability of the results, as the outcomes are intricately linked to physicochemical properties that are not well mapped. This study already highlights that ambient conditions should be considered in DAC optimisation. Including additional sorbents in the analysis once data is available would further enhance the level of detail but would not change the core finding.

3.5 Impact of on-site energy emissions on sorbent selection

As previously described in Section 3.3 and 3.4, two factors influence the choice of sorbent: first, the ambient conditions including how intensively they vary, and second, the on-site emissions of the energy used. During CRR optimisation, the on-site energy emissions are decisive in determining whether higher energy consumption for desorption is reasonable. As shown in Fig. 10, varying the on-site energy emissions from $0 \text{ kg kW}^{-1} \text{ h}^{-1} = 0 \text{ kg MJ}^{-1}$ to $0.3 \text{ kg kW}^{-1} \text{ h}^{-1} = 0.0833 \text{ kg MJ}^{-1}$ leads to different optimal sorbents, even under the same ambient conditions (resampled data for Calgary and Barbados).

Calgary yields high relative humidity at low temperatures, which, under the default on-site emissions, favours SIFSIX. However, reducing on-site emissions shifts the preference to NbOFFIVE. This is because NbOFFIVE captures more CO_2 than

SIFSIX, albeit with greater H_2O adsorption. Lowering the on-site emissions of the energy used means that desorbing additional H_2O results in fewer on-site emissions, leading to a higher CRR. When on-site energy emissions exceed the value of $0.24 \text{ kg kW}^{-1} \text{ h}^{-1}$, APDES becomes preferable. This result may seem counter-intuitive since APDES is typically considered optimal only under warm and humid conditions, suggesting it should not be the best sorbent for a location like Calgary. However, to reduce on-site emissions, the DAC system aims to minimise its energy consumption. Sensible heat losses from heating the sorbent notably contribute to the DAC system's energy demand.²⁶ APDES has a much lower density than SIFSIX (61 kg m^{-3} vs. 786 kg m^{-3}), meaning that for a fixed volume, less mass of sorbent needs to be heated. This consumes less energy for sensible heating, thereby reducing on-site emissions and supporting the decision to change the sorbent material.

The impact of reduced energy demands is also reflected by the extended cycle duration. With the same sorbent, higher on-site energy emissions consistently lead to longer cycle times, reducing the number of heating cycles and, consequently, sensible heat losses. Conversely, with low on-site energy emissions, the cycle design is shorter, allowing for more frequent adsorption/desorption cycles and capturing more CO_2 , as the penalties for heating and cooling are less severe.

The results also indicate that, in Barbados, due to its high humidity, the optimal sorbent remains unchanged, with APDES consistently performing best. However, when on-site emissions exceed the default value, the influence of ambient conditions on sorbent selection diminishes, as the DAC system focuses on minimising its energy demand to reduce sensible heat losses.

4 Conclusions

This study aims to achieve two main objectives: to examine the impact of hourly changing ambient conditions on the optimal sorbent selection for DAC and to explore the potential for reducing 1-D DAC models to a computationally efficient, simplified, time-dependent, 0-D model.

Previous studies investigated DAC performance under constant ambient conditions and considered only one sorbent. While these studies offered insights into the optimisation of DAC systems, the results in this study demonstrate that there are limitations to this previous approach. First, assuming constant ambient conditions leads to an inaccurate description of DAC systems dynamics, as varying ambient conditions notably impact sorbent performance. Second, optimising DAC for a single sorbent in one location does not yield the best possible results as adjusting sorbent selection according to ambient conditions can further improve performance. These two factors, therefore, emphasise that optimising DAC systems with only one sorbent under constant ambient conditions does not necessarily yield optimal results. Finally, this study recommends that future decision-making should account for multiple sorbents and hourly changing ambient conditions.

1-D models are widely used in the literature, but optimising them for hourly changing ambient conditions across various global locations demands considerable computational

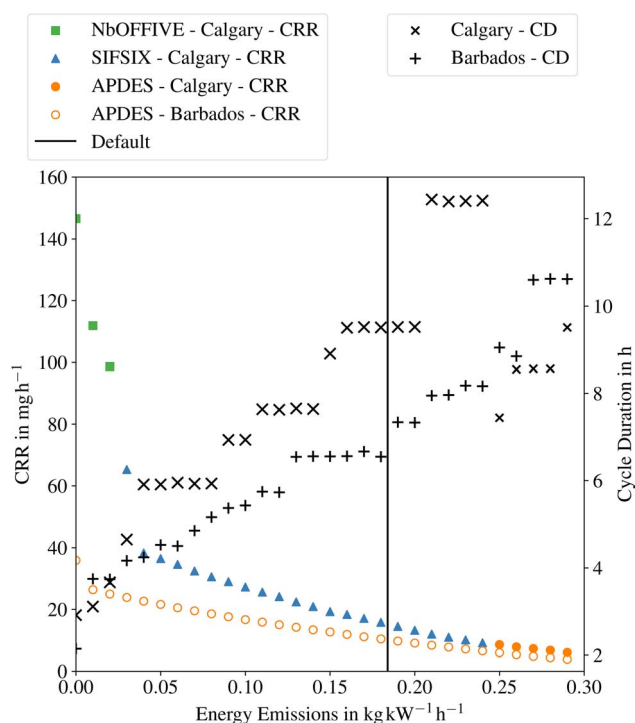


Fig. 10 Influence of on-site energy emissions on optimal sorbent selection and cycle duration (CD) for Calgary and Barbados, using resampled ambient conditions.



resources. Simplifying the 1-D model to a time-dependent 0-D model can reduce these computational costs while still yielding accurate results. This study demonstrates that such simplification is feasible, with 0-D model results and main KPIs closely aligned with the 1-D model. Ultimately, a major contribution of this study is that the simplification advances the broader academic understanding of DAC. The 0-D model allows for future investigations that are faster and less reliant on high-performance computing clusters, thereby expanding the accessibility of DAC modelling to a wider audience.

This study provides a framework for integrating multiple sorbents and hourly changing ambient conditions into the analysis and focuses on providing qualitative guidelines for sorbent selection. That said, data limitations restrict its ability to provide accurate, absolute estimates of DAC system performance. For example, the relative paucity of experimental equilibrium and kinetic data introduces a high degree of uncertainty, particularly in assumptions regarding heat and mass transfer or the impact of water and steam on system performance. Additionally, different sorbents exhibit varying material properties, particularly with respect to mass transfer, stability, oxidative degradation, and other factors. While it is acknowledged that these characteristics also affect sorbent selection, reliable data for these parameters are not available for the sorbents considered in this study. Nonetheless, this work demonstrates that, in addition to intrinsic material properties, the choice of sorbent is also influenced by the ambient conditions during DAC operation. Furthermore, using the CRR as the objective function has disadvantages, as it is an extensive property tied to the fixed size of the system, making comparisons with other NETs difficult. To mitigate this, the incorporation of costs in DAC optimisation is gaining traction in the literature, as the cost per ton of captured CO₂ allows for objective comparisons across different technologies. However, this approach is not part of the current study. Additionally, modelling assumptions and the choice of model structure introduce uncertainty, as no model perfectly represents real-world conditions. Regardless of using a 1-D or 0-D model, quantitative differences from real-world systems are expected. Such discrepancies are inherent, as all models approximate reality but cannot capture its full complexity. For example, one such limitation is the simplification of contactor geometry, overlooking the complex heat and mass transfer processes it entails.

To conclude, this study presents a new framework that serves as a building block for simplifying the understanding of DAC, one of several climate change mitigation technologies. The framework is straightforward and quick to apply, yielding sufficiently accurate DAC modelling that can be integrated into other models. Consequently, it can support global analysis of DAC systems under hourly changing ambient conditions, potentially aiding future research on optimal DAC site selection. Suggested future studies can focus on a more comprehensive evaluation of DAC performance, including its integration into the broader energy system and storage opportunities, as well as life-cycle assessment (LCA) and techno-economic assessment (TEA). Additionally, more data on sorbent performance is

required to improve the robustness of the model's results. Once the data is available, it can be easily integrated into the current framework, thanks to the modularity of the 0-D model, which allows for rapid re-evaluation. When combined with a more thorough analysis, including LCA and TEA, this approach will enable the development of realistic scenarios for DAC integration and application.

Data availability

This study was carried out using publicly available data from the Global Modeling and Assimilation Office (GMAO).

Author contributions

Malte Glaser: conceptualisation, data curation, formal analysis, methodology, software, validation, visualisation, writing – original draft. Arvind Rajendran: conceptualisation, methodology, writing – review & editing. Sean T. McCoy: conceptualisation, funding acquisition, methodology, project administration, resources, supervision, writing – review & editing.

Conflicts of interest

There are no conflicts to declare.

Acknowledgements

This work is an output of the CanCO₂Re project. This project was undertaken with the financial support of the Government of Canada. We would also like to thank Bhushesh Murugappan Balasubramaniam for his support in helping to interpret his previously published work, as well as for the helpful discussions and ongoing assistance throughout this research.

References

- 1 *Climate Change 2022 – Mitigation of Climate Change*, ed. Intergovernmental Panel on Climate Change (Ipcc), Cambridge University Press, 1st edn, 2023, pp. 3–48.
- 2 J. G. Shepherd, K. Caldeira, P. Cox, J. Haigh, D. Keith, B. E. Launder, G. Mace, G. MacKerron, J. Pyle, S. Raynor, C. Redgwell and A. Watson, *Geoengineering the Climate: Science, Governance and Uncertainty*, Royal Society, London, 2009.
- 3 M. J. Gidden, S. Roe, G. Ganti, T. Gasser, T. Hasegawa, W. F. Lamb, Y. Ochi, J. Streffer and N. E. Vaughan, Chapter 8: Paris-consistent CDR scenarios, in *The State of Carbon Dioxide Removal*, ed. S. M. Smith *et al.*, 2nd edn, 2024, DOI: [10.17605/OSF.IO/8XK7H](https://doi.org/10.17605/OSF.IO/8XK7H), <https://www.stateofcdr.org>.
- 4 T. Gasser, C. Guivarch, K. Tachiiri, C. D. Jones and P. Ciais, *Nat. Commun.*, 2015, **6**, 7958.
- 5 Ipcc, *Global Warming of 1.5 °C: IPCC Special Report on Impacts of Global Warming of 1.5 °C above Pre-industrial Levels in Context of Strengthening Response to Climate Change*,



- Sustainable Development, and Efforts to Eradicate Poverty*, Cambridge University Press, 1st edn, 2022.
- 6 J. C. Minx, W. F. Lamb, M. W. Callaghan, S. Fuss, J. Hilaire, F. Creutzig, T. Amann, T. Beringer, W. De Oliveira Garcia, J. Hartmann, T. Khanna, D. Lenzi, G. Luderer, G. F. Nemet, J. Rogelj, P. Smith, J. L. Vicente Vicente, J. Wilcox and M. Del Mar Zamora Dominguez, *Environ. Res. Lett.*, 2018, **13**, 063001.
 - 7 UNFCCC, *Paris Agreement to the United Nations Framework Convention on Climate Change*, 2015.
 - 8 S. E. Tanzer and A. Ramirez, *Energy Environ. Sci.*, 2019, **12**, 1210–1218.
 - 9 S. Cobo, V. Negri, A. Valente, D. M. Reiner, L. Hamelin, N. M. Dowell and G. Guillén-Gosálbez, *Environ. Res. Lett.*, 2023, **18**, 023001.
 - 10 H. Jung, K. Kim, J. Jeong, A. Jamal, D.-Y. Koh and J. H. Lee, *Chem. Eng. J.*, 2025, **508**, 160840.
 - 11 S. Jamdade, X. Cai, M. R. Allen-Dumas and D. S. Sholl, *ACS Sustainable Chem. Eng.*, 2024, **12**, 16680–16691.
 - 12 M. Sendi, M. Bui, N. Mac Dowell and P. Fennell, *One Earth*, 2022, **5**, 1153–1164.
 - 13 J. F. Wiegner, A. Grimm, L. Weimann and M. Gazzani, *Ind. Eng. Chem. Res.*, 2022, **61**, 12649–12667.
 - 14 L. Grazia, S. Fennell Paul and S. Nilay, *Chem. Eng. Trans.*, 2022, **96**, 1–6.
 - 15 X. Cai, M. A. Coletti, D. S. Sholl and M. R. Allen-Dumas, *JACS Au*, 2024, **4**, 1883–1891.
 - 16 H. M. Schellevis, J. D. De La Combé and D. W. F. Brilman, *Energy Adv.*, 2024, **3**, 1678–1687.
 - 17 P. Postweiler, M. Engelpracht, D. Rezo, A. Gibelhaus and N. Von Der Assen, *Energy Environ. Sci.*, 2024, **17**, 3004–3020.
 - 18 A. Luukkonen, J. Elfving and E. Inkeri, *Chem. Eng. J.*, 2023, **471**, 144525.
 - 19 H. Schellevis, T. Van Schagen and D. Brilman, *Int. J. Greenh. Gas Control*, 2021, **110**, 103431.
 - 20 F. Sabatino, A. Grimm, F. Gallucci, M. Van Sint Annaland, G. J. Kramer and M. Gazzani, *Joule*, 2021, **5**, 2047–2076.
 - 21 E. S. Sanz-Pérez, C. R. Murdock, S. A. Didas and C. W. Jones, *Chem. Rev.*, 2016, **116**, 11840–11876.
 - 22 M.-Y. A. Low, L. V. Barton, R. Pini and C. Petit, *Chem. Eng. Res. Des.*, 2023, **189**, 745–767.
 - 23 V. Stampi-Bombelli, M. Van Der Spek and M. Mazzotti, *Adsorption*, 2020, **26**, 1183–1197.
 - 24 J. Young, E. García-Díez, S. Garcia and M. Van Der Spek, *Energy Environ. Sci.*, 2021, **14**, 5377–5394.
 - 25 X. Zhu, T. Ge, F. Yang and R. Wang, *Renew. Sustain. Energy Rev.*, 2021, **137**, 110651.
 - 26 B. M. Balasubramaniam, P.-T. Thierry, S. Lethier, V. Pugnet, P. Llewellyn and A. Rajendran, *Chem. Eng. J.*, 2024, **485**, 149568.
 - 27 V. Subramanian Balashankar, A. K. Rajagopalan, R. De Pauw, A. M. Avila and A. Rajendran, *Ind. Eng. Chem. Res.*, 2019, **58**, 3314–3328.
 - 28 Low-Pressure Drop Structure Of Particle Adsorbent Bed For Adsorption Gas Separation Process, 2014, <https://patentscope.wipo.int/search/en/detail.jsf?docId=WO2014170184>.
 - 29 A. R. Kulkarni and D. S. Sholl, *Ind. Eng. Chem. Res.*, 2012, **51**, 8631–8645.
 - 30 R. Haghpanah, A. Majumder, R. Nilam, A. Rajendran, S. Farooq, I. A. Karimi and M. Amanullah, *Ind. Eng. Chem. Res.*, 2013, **52**, 4249–4265.
 - 31 C. Gebald, J. A. Wurzbacher, A. Borgschulte, T. Zimmermann and A. Steinfeld, *Environ. Sci. Technol.*, 2014, **48**, 2497–2504.
 - 32 S. Mukherjee, N. Sikdar, D. O’Nolan, D. M. Franz, V. Gascón, A. Kumar, N. Kumar, H. S. Scott, D. G. Madden, P. E. Kruger, B. Space and M. J. Zaworotko, *Sci. Adv.*, 2019, **5**, eaax9171.
 - 33 Global Modeling and Assimilation Office and S. Pawson.
 - 34 M. Hoffmann, L. Kotzur and D. Stolten, *Appl. Energy*, 2022, **315**, 119029.
 - 35 T. Pandas Development Team, *Pandas-Dev/pandas: Pandas*, 2020, DOI: [10.5281/zenodo.3509134](https://doi.org/10.5281/zenodo.3509134).
 - 36 P. Virtanen, R. Gommers, T. E. Oliphant, M. Haberland, T. Reddy, D. Cournapeau, E. Burovski, P. Peterson, W. Weckesser, J. Bright, S. J. van der Walt, M. Brett, J. Wilson, K. J. Millman, N. Mayorov, A. R. J. Nelson, E. Jones, R. Kern, E. Larson, C. J. Carey, Í. Polat, Y. Feng, E. W. Moore, J. VanderPlas, D. Laxalde, J. Perktold, R. Cimrman, I. Henriksen, E. A. Quintero, C. R. Harris, A. M. Archibald, A. H. Ribeiro, F. Pedregosa, P. van Mulbregt and SciPy 1.0 Contributors, *Nat. Methods*, 2020, **17**, 261–272.
 - 37 SEAI, Conversion and Emission Factors for Publication, 2023, <https://www.seai.ie/data-and-insights/seai-statistics/conversion-factors/>.
 - 38 J. Blank and K. Deb, *IEEE Access*, 2020, **8**, 89497–89509.
 - 39 The Reality of Deploying Carbon Removal via Direct Air Capture in the Field, 2024, <https://climeworks.com/news/the-reality-of-deploying-direct-air-capture-in-the-field>.

